Ceramics-Silikáty 60 (2), 122-128 (2016)
journal webpage: www.ceramics-silikaty.cz doi: 10.13168/cs.2016.0018

INFLUENCE OF MnO_2 ADDITIONS TO $BaNd_2Ti_4O_{12}$ MICROWAVE CERAMICS ON SINTERING BEHAVIOR AND DIELECTRIC PROPERTIES

ZI-XUAN FANG, #BIN TANG, MING-ZHU LONG, SHU-REN ZHANG

School of Microelectronics and Solid State Electronics, University of Electronic Science and Technology of China, Chengdu 610054, People's Republic of China
National Engineering Center of Electromagnetic Radiation Control Materials, University of Electronic Science and Technology of China, Jianshe Road, Chengdu 610054, PR China

#E-mail: tangbin@uestc.edu.cn

Submitted October 14, 2015; accepted March 2, 2016

Keywords: $BaNd_2Ti_4O_{12}$, Microwave ceramics, Dielectric properties, Microstructure

The sintering behaviors and microwave dielectric properties of $BaNd_2Ti_4O_{12}$ (BNT4) ceramics with x wt. % MnO_2 dopants (x = 0, 1, 2, 3 and 4) were investigated in this paper. The tungsten–bronze type $BaNd_2Ti_4O_{12}$ accompanied with a certain amount of $Ba_2Ti_9O_{20}$ secondary phase was observed for all Mn doped compositions when samples were sintered at 1300°C. Manganese substitution for Ti caused a decrease of the lattice parameters, and the addition of MnO_2 effectively improved the densification and lowered the sintering temperature of ceramics, which was closely related to the liquid phase sintering mechanism. The microstructure was homogeneous fine grained when x equaled to 3. At last, the $BaNd_2Ti_4O_{12}$ with 3.0 wt. % MnO_2 dopants well-sintered at 1300°C for 1 h had good microwave dielectric properties of ε_r = 90.2, $Q \times f$ = 5225 GHz and τ_f = 9.7 ppm·°C^{-1}.

INTRODUCTION

With the explosively increasing demand in the wireless communication systems and consumer electronic market, the microwave dielectric ceramics have been extensively investigated for microwave device applications, such as resonators, filters, and oscillators [1, 2]. Among tremendous amounts of microwave dielectric materials, $BaO–Ln_2O_3–TiO_2$ (Ln = Nd, Sm and La) are attracting much attention because of their high dielectric constants (ε_r = 80 – 110), high quality factors ($Q \times f$ = 1 800 ~ 10 000 GHz) and tunable temperature coefficients of resonant frequency (τ_f) [3]. Ceramics, with $BaO:Nd_2O_3:TiO_2$ of around 1:1:4 and a high dielectric constant (ε_r = 70 – 90), have been commonly applied in mobile telephone systems [4]. As reported by previous researches [4, 5], the chemical compound $BaNd_2Ti_4O_{12}$ has emerged as a promising microwave ceramic due to a good combination of a high dielectric constant (ε_r ~ 84) and a high quality factor ($Q \times f$ ~ 7 800 GHz). But the large τ_f value of 94 ppm·°C^{-1} limits its practical applications as dielectric resonator.

Fortunately, recent studies reported that Mn^{4+} or Mn^{2+} ions had positive effect on the dielectric properties of various ceramics. The MnO_2 is an effective sintering aid to enhance densification and reduce dielectric loss in $Ba_{4.2}Nd_{9.2}Ti_{18}O_{54}$-$NdAlO_3$ and $K_{0.5}Na_{0.5}Nb_{0.92}Sb_{0.08}O_3$ system [6, 7]. As the critical concentration (≥ 43 mol. %) of $MnCO_3$ additives was reached, Lee et al. [8]. revealed that the microwave dielectric properties of $BaO–(Nd_{0.7}Sm_{0.3})_2O_3–4TiO_2$ were significantly improved owing to the formation of a new $BaNd_2Ti_4O_{12}$ phase and a Mn-rich phase. Varma et al. [9]. reported that an improved quality factor of $Ba(Zn_{1/3}Ta_{2/3})O_3$ ceramics was obtained with a small amount of MnO_2. Cai et al. [10] studied the dielectric properties of $BaZr_{0.2}Ti_{0.8}O_3$ ceramics doped by various concentration of MnO_2. It was found that Mn^{4+} ions had entered the unit cell occupying the B sites of the perovskite structure and with increasing MnO_2 addition, the dielectric loss of $BaZr_{0.2}Ti_{0.8}O_3$ ceramics could be effectively reduced.

So far, many efforts have been made to improve the comprehensive properties of $BaNd_2Ti_4O_{12}$ ceramics by doping various additives. CuO can effectively reduce the sintering temperature with a small amount of addition, so that the negative impact of sintering aid on dielectric properties such as quality factor can be minimized [5]. It was also reported by Chen et al. that an increasing dielectric constant and a near-zero τ_f value were obtained by doping $Bi_4B_2O_9$ to BNT4 ceramics [11]. However, MnO_2, as an effective aid to many material systems, has not been systematically researched in BNT4 ceramics. In our present work, the effects of various contents of MnO_2 additives on microstructure, sintering behavior and microwave dielectric properties of $BaNd_2Ti_4O_{12}$ were investigated in detail.

EXPERIMENTAL

The $BaNd_2Ti_4O_{12}$ microwave ceramics were synthesized by the conventional solid-state ceramic route. High-purity powders of $BaCO_3$ (≥ 99.9 %, Mianyang Yuanda New Materials Co., Ltd, Mianyang, China), Nd_2O_3 (99.8 %, Gansu Rare-earth New Materials Co., Ltd, Baiyin, China), MnO_2 (99.8 %, Xiantao ZhongXing Electric Co., Ltd, Xiantao, China) and TiO_2 (99.9 %, Xiantao ZhongXing Electric Co., Ltd, Xiantao, China) were used as the starting materials. The raw oxide materials were weighed according to the stoichiometry proportions and ball milled in deionized water medium for 5 h in nylon jars using zirconia balls. The mixture was dried and calcined at 1100°C for 4 h. Then the calcined BNT4 powders were re-milled respectively with x wt. % MnO_2 (x = 1, 2, 3 and 4) powders for 4 h. After drying, the powder was mixed with 5 wt. % polyvinyl alcohol (PVA) binder, then dried and ground well. The obtained fine powder was axially pressed into cylindrical disks with the thickness of 4 mm and 11 mm in diameter under a pressure of 25 MPa. These pellets were sintered at different sintering temperatures from 1200 to 1350°C for 1 h in air.

After sintering, the bulk densities of the samples were measured using the Archimedes method. The phase composition and crystal structure of the ceramics were examined by X-ray diffraction technique using CuKa radiation (DX–1000 CSC, Japan). Scanning electron microscopy (SEM) (JSM-6460LV, Jeol, Tokyo, Japan) was employed to study the surface morphology of the specimens. The microwave dielectric properties were measured by a Vector Network Analyzer (E5071C, Agilent Technologies) and a temperature chamber (DELTA 9023, Delta Design, USA.). In addition, the temperature coefficients of resonant frequency τ_f values were calculated by the equation: $\tau_f = (f_{t_2} - f_{t_1})/[f_{t_1} \times \times (t_2 - t_1)]$, where f_{t_1} and f_{t_2}, were the resonant frequencies at the measuring temperature t_1 (25°C) and t_2 (85°C), respectively.

RESULTS AND DISCUSSION

Figure 1a shows the XRD patterns of $BaNd_2Ti_4O_{12}$ ceramics with different x value sintered at 1300°C for 1 h in air. For the sintered samples of all compositions, the main phase was identified as orthorhombic tungsten–bronze type $BaNd_2Ti_4O_{12}$ (JCPDS Card No. 44-0061). However, it was also observed that a certain amount of $Ba_2Ti_9O_{20}$ secondary phase (JCPDS Card No.76-1538) appeared with $x \geq 1$ wt. %. Obviously, with 1 wt. % MnO_2 addition, the diffraction peak of the main crystal phase $BaNd_2Ti_4O_{12}$ showed the strongest intensity, which indicated that $BaNd_2Ti_4O_{12}$ crystals grew better than in other compositions. As the amount of MnO_2 was increased, the diffraction intensity of $BaNd_2Ti_4O_{12}$ phase weakened sharply. Especially for the composition with x = 4 wt. %, the diffraction intensity of its main phase was nearly three fourths of that for the composition with x = 1 wt. %. In order to clarify the peaks of the secondary phase, the amplified profiles (a) of strongest characteristic peak (around the 2θ angle of 28.9°) for the $Ba_2Ti_9O_{20}$ phase of the corresponding specimens are shown in Figure 1b. As displayed in Figure 1b, it was clear that the amount of $Ba_2Ti_9O_{20}$ phase remained almost the same accompanied by the decreasing intensity of main phase with an increase of MnO_2 content. As reported in previous researches [12, 13], the anorthic $Ba_2Ti_9O_{20}$ secondary phase was frequently found in variously doped $BaO–Ln_2O_3–TiO_2$ ceramics even in the pure $BaO–Ln_2O_3–TiO_2$ system ceramic. Fortunately, under our experimental conditions, no other impurity phases were detected in the pure BNT4 ceramics (x = 0 wt. %). Finally, it was known that the decrease of main crystal phase content would have a significant influence on the dielectric properties of microwave ceramics.

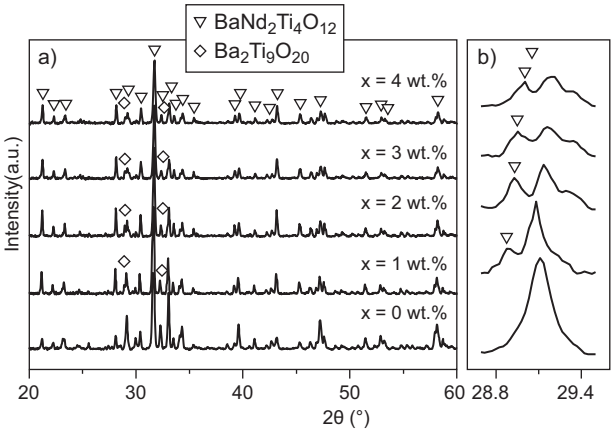

Figure 1. XRD patterns of $BaNd_2Ti_4O_{12}$ samples with different x value sintered at 1300°C for 1 hour in air (a); the strongest peak (around the 2θ angle of 28.9°) for the $Ba_2Ti_9O_{20}$ phase of the corresponding specimens (b).

It was also found from Figure 1a and Figure 1b that there was a movement of the peaks towards higher degree for $BaNd_2Ti_4O_{12}$ phase indicating smaller ionic substitution according to Bragg's law. Hence the lattice parameters and unit cell volume for the solid solution $BaNd_2Ti_4O_{12}$ phase were calculated and the results are shown in Figure 2. With increasing the doping amount of MnO_2 from 1 wt. % to 4 wt. %, the a-axis, b-axis and c-axis were dropped, and thus the unit cell volume also declined. It was deduced that Mn^{4+} ions inclined to partially substitute for Ti^{4+} of $BaNd_2Ti_4O_{12}$ ceramics and form a solid solution, since the ionic radius of Mn^{4+} (0.60 Å) is close to that of Ti^{4+} (0.68 Å) and much smaller than that of Ba^{2+} (1.34 Å) and Nd^{3+} (1.04 Å) [14]. It was reported that Mn^{4+} had entered the unit cell occupying the Ti sites of the perovskite structure in $BaZr_{0.2}Ti_{0.8}O_3$ ceramics [10] and would exactly locate at the Ti site

in manganese doped $PbTiO_3$ ceramics [15]. From the continuous downward trend of lattice parameters as shown in Figure 2, it could be concluded that the amount of Ti^{4+} substituted by Mn^{4+} increased with increasing MnO_2 dopants and this substitution could cause the shrinkage of the crystal lattice for $BaNd_2Ti_4O_{12}$ ceramics. Moreover, since the part of Mn^{4+} entered into the crystal lattice would cause lattice distortion [16], the difference of their ionic radius also resulted in the lattice distortion.

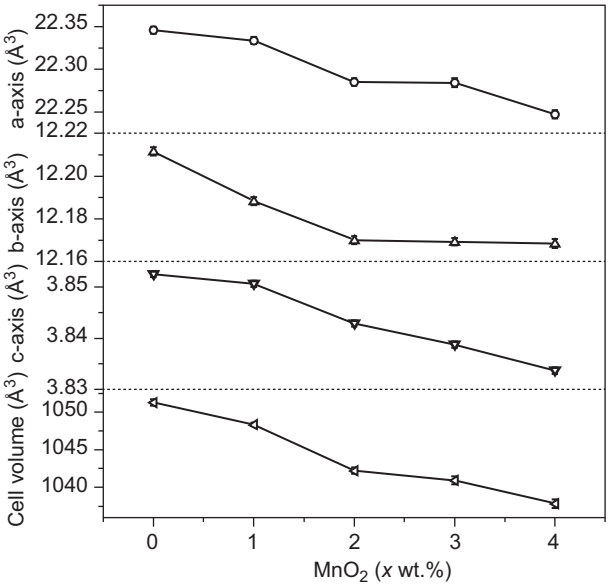

Figure 2. The MnO_2 doping dependence of the refined lattice parameters of $BaNd_2Ti_4O_{12}$ ceramics sintered at 1300°C for 1 h in air.

Figure 3 shows the SEM micrographs of $BaNd_2Ti_4O_{12}$ ceramics with various amounts of MnO_2 addition sintered at 1300°C for 1 h in air. We could see that the whole grains were long-column-like For the Mn-free samples (Figure 3a), the ceramic showed a porous and inhomogeneous microstructure, and had a grain size of 2 to 3 μm. For the samples doped with Mn additives (Figure 4b-e), the grain sizes in the range of 5 to 9 μm are much larger than those of Mn-free samples and it was evident that the grains gradually became larger and larger. And specimens with Mn additives presented compact microstructure with almost no pores, indicating that BNT4 samples with high densification were obtained. Increase of MnO_2 additive content had insignificant effect on the morphology of grains. But by careful observation of the microstructure, there indeed existed slight changes in the microstructure of grains. While increasing MnO_2 content up to 3 wt. %, the microstructures of BNT4 ceramics became more and more homogeneous, especially for the composition of 3 wt. %, the homogeneous fine grained microstructure was observed and the crystal grain size was in the range of 5 μm. Samples with 4 wt. % MnO_2 dopants also showed relatively uniform microstructure. But as directed by the white arrows in Figure 3e, it could be seen that the grain edge and corner became blurred when compared with those of other compositions.

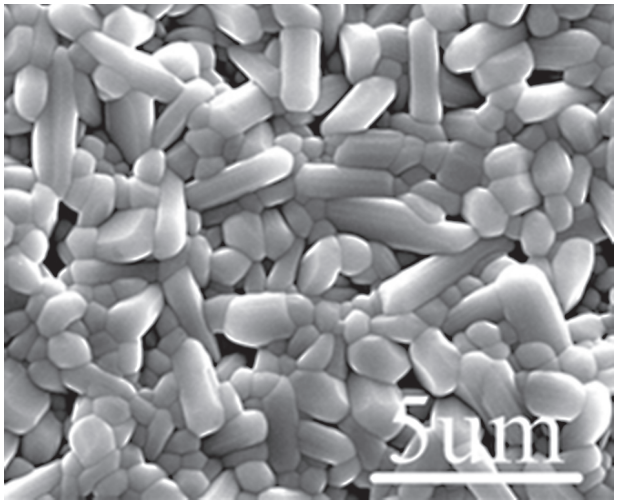

a)

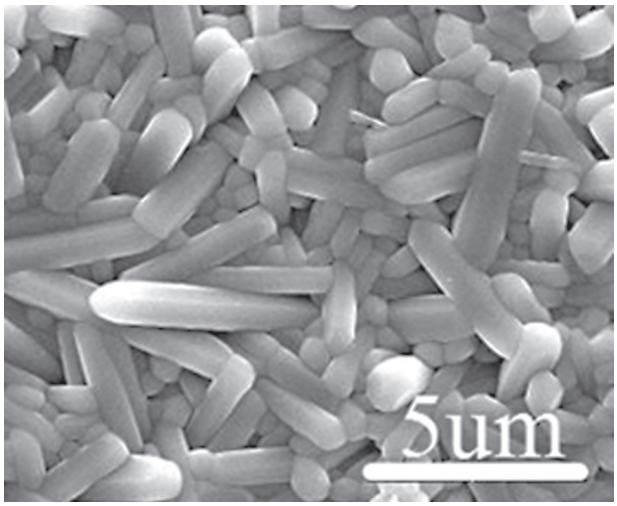

b)

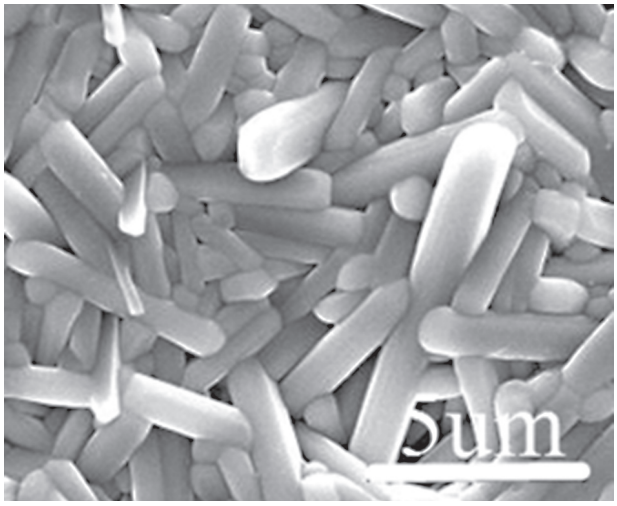

c)

Figure 3. The SEM micrographs of $BaNd_2Ti_4O_{12}$ ceramics with different *x* value sintered at 1300°C for 1 hour in air.

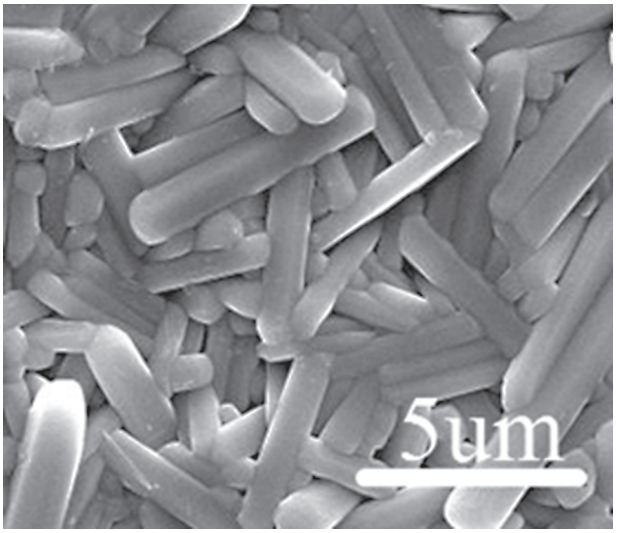

d)

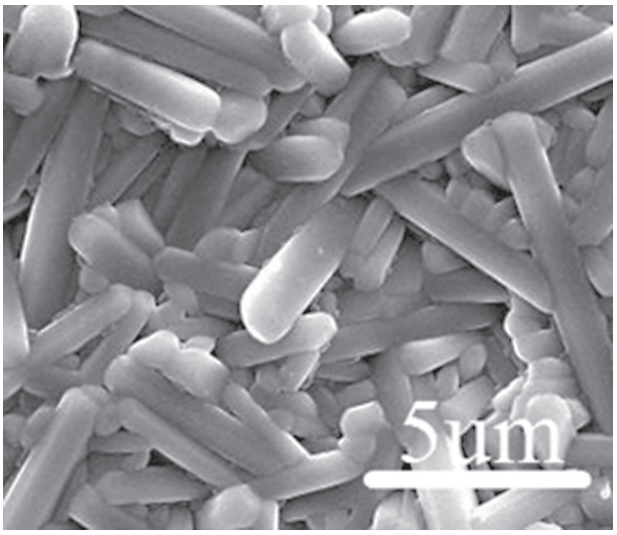

e)

Figure 3. The SEM micrographs of $BaNd_2Ti_4O_{12}$ ceramics with different *x* value sintered at 1300°C for 1 hour in air.

Figure 4 depicts the relative density of $BaNd_2Ti_4O_{12}$ ceramics with different MnO_2 addition content as a function of sintering temperature in air. It was obvious that as MnO_2 content varied from 0 wt. % to 2 wt. %, the relative density of samples with each fixed MnO_2 dopant maintained an upward trend due to the improvement of densification with increasing sintering temperature up to 1350°C. Meanwhile, in the relatively low sintering temperature range 1200 - 1300°C, the relative density was also strongly influenced by MnO_2 content. For example, as the MnO_2 content approached 3 wt. %, it can be seen that the relative density of BNT4 ceramics went up to the maximum value at 1300°C which was attributed to the improvement of densification, and thereafter decreased with further increase of sintering temperature. When the MnO_2 addition content was raised to 4 wt. %, the optimal sintering temperature can be effectively lowered to 1250°C. Also, in the low sintering temperature range of 1250°C to 1300°C, especially for the point of 1250°C, relative densities of Mn doped samples were significantly improved and much larger than that of Mn-free specimens. Laffez et al. [13] reported that MnO_2 dopants could form liquid phase in $Ba_{6-x}(Sm_{1-y}Nd_y)_{8+2x/3}Ti_{18}O_{54}$ oxides. Appel et al. [17] revealed that Mn doping promoted the propagation of ions because of the formation of Mn containing liquid phase at a lower sintering temperature of 1350°C. And as marked by white arrows in Figure 3d, the grains with blurred edge or corner may be related to the low melting compounds or liquid phase. Hence, by analogy, the sintering behavior of our experiment should be closely related to Mn doping causing the formation of Mn containing liquid phase. As previously reported [5], the optimal sintering temperature of pure $BaNd_2Ti_4O_{12}$ ceramics was generally higher than 1350°C. Therefore, when comparing our results with previous studies, we could clearly see that the adequate Mn doping would effectively reduce the sintering temperature and the BNT4 ceramics could be well-sintered at the temperature lower than 1300°C. And at low sintering temperature, relative densities of BNT4 samples could be significantly improved by the adding MnO_2.

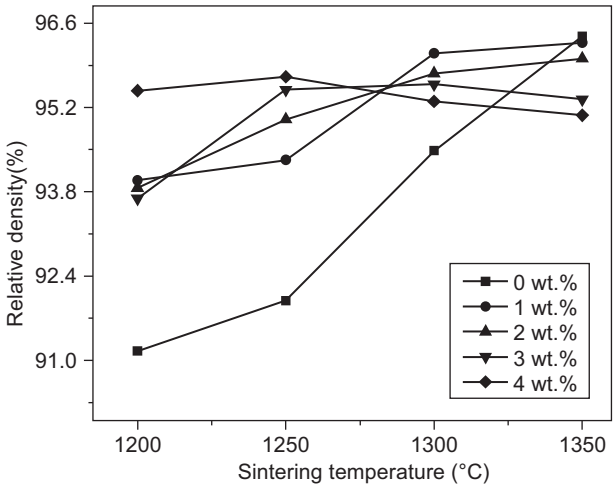

Figure 4. The relative density of $BaNd_2Ti_4O_{12}$ ceramics with different *x* value as a function of sintering

Figure 5 shows the dielectric constant of $BaNd_2Ti_4O_{12}$ ceramics with different MnO_2 doping content as a function of sintering temperature in air. The dielectric constant at microwave frequencies is dependent on the relative density, secondary phase, microstructure and polarizability [18, 19]. With MnO_2 contents varying from 0 wt. % to 3 wt. %, variation of the dielectric constant shown in Figure 5 was almost in accordance with that of the relative density presented in Figure 4 because both density and dielectric constant are strongly influenced by the fraction of pores (density ≈ 0 and $\varepsilon_r \approx 1$). When *x* equaled to 4 wt. %, the ε_r value increased first, reached a maximum value at 1300°C and then

decreased. The increase of ε_r value for specimens with $x = 4$ wt. % sintered below 1300°C was mainly attributed to the improvement of densification. As confirmed by the analysis of changing density, samples with 4 wt. % MnO_2 could be well-sintered at a much lower temperature of 1250°C. Therefore, it was reasonable to understand that the dielectric constant began to drop at the temperature above 1300°C which may be resulted from excessively high sintering temperature. Furthermore, the dielectric constant was strongly affected by the variation of MnO_2 dopants. When the amounts of MnO_2 dopants varied from 0 wt. % to 4 wt. %, the maximum ε_r value of every composition was raised from 75.2 to 93.0. First of all, the enhancement of ε_r could be attributed to the facts that uniform and oligoporous microstructures could be obtained for the compositions with 3 wt. % and 4 wt. % MnO_2, as shown in Figure 3d and Figure 3e. What's more, especially in the low sintering temperature of 1250°C to 1300°C, the dielectric constant was remarkably enhanced to the largest value of 93.0 which should primarily be contributed to the significant improvement of relative densities (from 91.2 % to 96.1 %). From another point of view, the number of polarizable particles per unit volume was increased due to the shrinkage of the cell volume, leading to the enhancement of polarizability [20-22]. Therefore, the successive shrinkage of the cell volumes caused by Mn^{4+} substitution might be responsible for the continuous improvement of dielectric constant with 1 wt. % ≤ x ≤ 4 wt. %. But for the Mn-doped BNT4 ceramics, our results indicated that the secondary phase failed to affect the dielectric constant although a certain amount of $Ba_2Ti_9O_{20}$ phase with relatively low ε_r value of 39.8 [23] were detected which may be contributed to the reason that its negative effect was compensated by the positive factors mentioned above. Eventually, it was obtained that a maximum ε_r (~ 93) of BNT4 ceramics with 3 wt. % MnO_2 was much higher than that of the pure BNT4 ceramics (~ 75), which was similar to that of Bi_2O_3-doped BNT4 ceramics [12] and $Bi_4B_2O_9$-doped BNT4 ceramics [11].

The variation of $Q \times f$ values for $BaNd_2Ti_4O_{12}$ ceramic samples sintered in air at different sintering temperatures as a function of different x value are presented in Figure 6. It was observed that the $Q \times f$ value was increased till 1350°C with $x \leq 2$ wt. %. For the compositions with 3wt. % and 4wt. % MnO_2, the $Q \times f$ value reached its maximum value at a sintering temperature of 1300°C and then started to decline. The $Q \times f$ value was affected by many factors, such as pores, structure defects, densification, phase compositions, micromorphology and lattice distortion [24-26]. With increasing x value from 0 wt. % to 4 wt. %, the overall $Q \times f$ values showed a downward trend from 9367 to 4658 GHz. As confirmed by XRD analysis in Figure 1, the intensity of main phase decreased sharply, and therefore the decrease of the $Q \times f$ value was mainly caused by the progressively deteriorated $BaNd_2Ti_4O_{12}$ phase. A similar result was observed in the experiment conducted by Laffez et al. They found that MnO_2 dopants could form liquid phase in $Ba_{6-x}(Sm_{1-y}Nd_y)_{8+2x/3}Ti_{18}O_{54}$ oxides which was probably the ferroelectric or semiconductor with high dielectric loss [13], and the $Q \times f$ values of samples decreased. In the end, the lattice distortion caused by manganese substitution may also be responsible to the consecutive decrease of $Q \times f$ values.

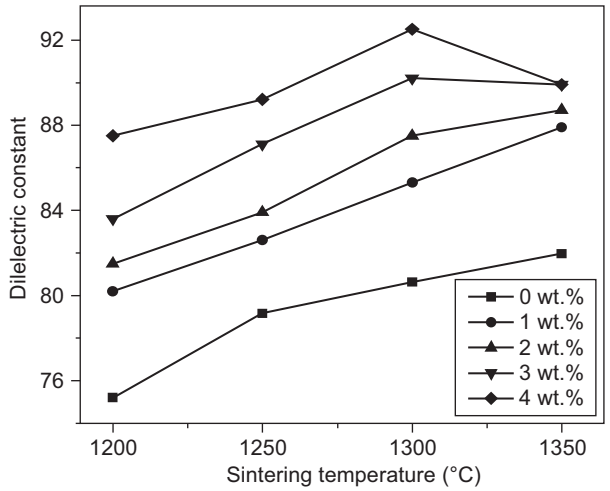

Figure 5. The dielectric constant of $BaNd_2Ti_4O_{12}$ ceramics with different x value as a function of sintering temperature for 1 hour in air.

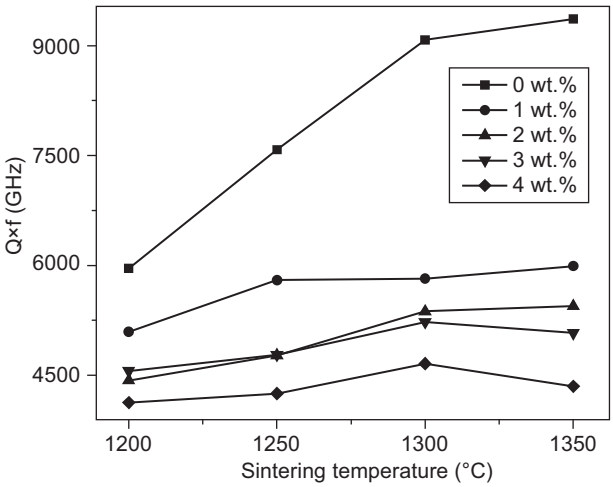

Figure 6. The quality factor of $BaNd_2Ti_4O_{12}$ ceramics with different x value as a function of sintering temperature

Figure 7 shows the temperature coefficient of the resonant frequency of $BaNd_2Ti_4O_{12}$ ceramics sintered in air at different temperatures as a function of the MnO_2 amounts. The τ_f values did not change considerably with 1 wt. % ≤ $x \leq 4$ wt. % and the overall τ_f values maintained an upward trend, which were between 7.7 and 14.2 ppm·°C^{-1}. It was remarkable that the τ_f values of MnO_2 added specimens were much lower than that of

pure BNT4 ceramics. In general, the τ_f is related to the composition, secondary phases [19], and crystal lattice [27]. The $Ba_2Ti_9O_{20}$ secondary phase was observed for all MnO_2 added samples. Hence, the appearance of $Ba_2Ti_9O_{20}$ probably contributed to the relatively lower τ_f values due to its much lower τ_f value of 2 ppm·°C^{-1} [23] when compared with the existed literature for $BaNd_2Ti_4O_{12}$ (τ_f = 94 ppm·°C^{-1}). Raising the amount of MnO_2 led to an increase of τ_f value. Kim et al. [28]. discovered that the τ_f of tungsten bronze-type structure was closely related to the extent of the tilting and distortion of the octahedron. When combining the analysis with Figure 2, doping MnO_2 could have an influence on the tilting and distortion of the octahedron in BNT4 ceramics. Therefore, it was reasonable to believe that τ_f value would move towards the positive direction when the BNT4 ceramics are doped with increasing content of MnO_2.

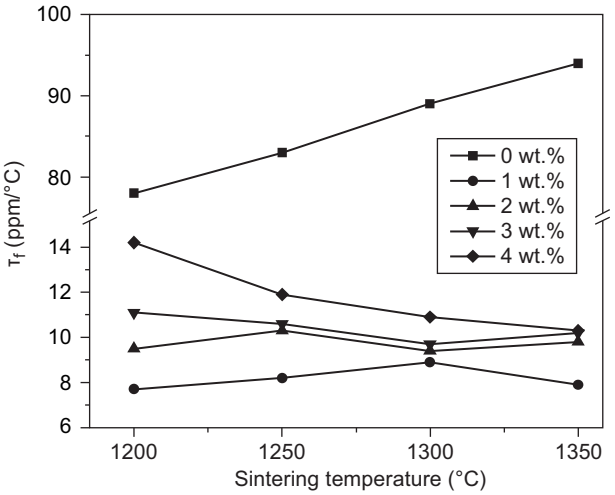

Figure 7. The temperature coefficients of resonant frequency of $BaNd_2Ti_4O_{12}$ ceramics with different *x* value as a function of sintering temperature for 1 hour in air.

Typically, 3 wt. % MnO_2-doped $BaNd_2Ti_4O_{12}$ ceramic sintered at 1300°C exhibited compact microstructure and good microwave dielectric properties of ε_r = 90.2, $Q \times f$ = 5225 GHz and τ_f = 9.7 ppm·°C^{-1}. In addition to a relatively low sintering temperature, $BaNd_2Ti_4O_{12}$ ceramics prepared by MnO_2 doping exhibited better and more stable microwave dielectric properties compared with that of pure $BaNd_2Ti_4O_{12}$ ceramics sintered at high sintering temperature of above1350°C [4, 5].

CONCLUSIONS

The addition of MnO_2 reduces the sintering temperature of $BaNd_2Ti_4O_{12}$ ceramics from 1350°C to 1250°C with the improvement of microwave dielectric properties. The tungsten–bronze type $BaNd_2Ti_4O_{12}$ accompanied with a certain amount of $Ba_2Ti_9O_{20}$ secondary phase was observed at all compositions when samples were sintered at 1300°C. The lattice constants and cell volumes of $BaNd_2Ti_4O_{12}$ ceramics kept decreasing with increasing amounts of MnO_2, which indicated that the Manganese substituted for Ti^{4+} in ceramic matrix and led to an shrinkage of the lattice. The changes in microwave dielectric properties were closely related to the trends in the crystal lattice and densification. A similar trend was observed between the relative density and ε_r value. With x ≤ 2.0 wt. %, the ε_r value increased obviously with increasing sintering temperature due to the improvement of densification. Typically, when x = 4.0 wt. %, a high ε_r value of 92.5 for ceramics sintered at 1300°C for 1 h was obtained. But the $Q \times f$ value decreased from 5990 to 4659 GHz with 1 wt. % ≤ x ≤ 4 wt. % due to the progressively deteriorated main phase and the appearance of liquid phase. Finally, the τ_f value increased with increasing MnO_2 content. Hence, 3 wt. % MnO_2-doped $BaNd_2Ti_4O_{12}$ ceramic sintered at 1300°C for 1 h exhibited compact microstructure and good microwave dielectric properties of ε_r = 90.2, $Q \times f$ = 5225 GHz and τ_f = 9.7 ppm·°C^{-1}.

Acknowledgments

This work is supported by National Natural Science Funds of China (Grant No. 51402039).

REFERENCES

1. Li Y., Li H., Li J., Tang B., Zhang S., Chen H., Wei Y. (2014): Effect of TiO_2 Ratio on the Phase and Microwave Dielectric Properties of $Li_2ZnTi_{3+x}O_{8+2x}$ Ceramics. *Journal of electronic materials*, *43*(4), 1107-1111. doi:10.1007/s11664-014-3026-4
2. Chen G.H., Yuan C.L., Zhou C.R., Yang Y. (2013): Low-firing high permittivity $Ca_{0.6}Sm_{0.8/3}TiO_3$–$(Li_{0.5}Nd_{0.5})TiO_3$ ceramics with BaCu (B_2O_5) addition. *Ceramics International*, *39*(8), 9763-9766. doi:10.1016/j.ceramint.2013.05.028
3. Nenasheva E. A., Kartenko N. F. (2001): High dielectric constant microwave ceramics. *Journal of the European Ceramic Society*, *21*(15), 2697-2701. doi:10.1016/S0955-2219(01)00348-X
4. Fu Y.P., Liu C. W., Lin C.H., Hsieh C.K. (2005): Effect of TiO_2 ratio on BaO–Nd_2O_3–TiO_2 microwave ceramics. *Ceramics international*, *31*(5), 667-670. doi:10.1016/j.ceramint.2004.08.005
5. Wu M.C., Hsieh M.K., Yen C.W., Huang Y.C., Huang W.T., Su W.F. (2007): Low sintering $BaNd_2Ti_4O_{12}$ microwave ceramics prepared by CuO thin layer coated powder. *Journal of the European Ceramic Society*, *27*(8), 2835-2839. doi:10.1016/j.jeurceramsoc.2006.11.057
6. Huang B., Wang Z., Chen T., Wang L., Fu Z., Zhang Q. (2014): Effects of MnO_2 doping on microstructure and microwave dielectric properties of $Ba_{4.2}Nd_{9.2}Ti_{18}O54$–$NdAlO_3$ ceramics. *Journal of Materials Science: Materials in Electronics*, *25*(12), 5264-5268. doi:10.1007/s10854-014-2299-y

7. Lin D., Zheng Q., Kwok K. W., Xu, C., Yang C. (2010): Dielectric and piezoelectric properties of MnO_2-doped $K_{0.5}Na_{0.5}Nb_{0.92}Sb_{0.08}O_3$ lead-free ceramics. *Journal of Materials Science: Materials in Electronics*, *21*(7), 649-655. doi:10.1007/s10854-009-9971-7
8. Lee W.H., Su C.Y., Lee Y.C. (2007): Mn-Doped BaO–$(Nd_{0.7}, Sm_{0.3})_2O_3$–$4TiO_2$ Ceramic Sintered in a Reducing Atmosphere. *Japanese journal of applied physics*, *46*(4R), 1562. doi:10.1143/JJAP.46.1562
9. Varma M.R., Raghunandan R., Sebastian M.T. (2005): Effect of dopants on microwave dielectric properties of Ba $(Zn_{1/3}Ta_{2/3})$ O_3 ceramics. *Japanese journal of applied physics*, *44*(1R), 298. doi:10.1143/JJAP.44.298
10. Cai W., Fu C., Gao J., Deng X. (2010): Effect of Mn doping on the dielectric properties of $BaZr_{0.2}Ti_{0.8}O_3$ ceramics. *Journal of Materials Science: Materials in Electronics*, *21*(4), 317-325. doi: 10.1007/s10854-009-9913-4
11. Chen X., Zhang W., Bai S. (2013): Effect of $Bi_4B_2O_9$ addition on the sintering temperature and microwave dielectric properties of BaO–Nd_2O_3–$4TiO_2$ ceramics. *Journal of Materials Science: Materials in Electronics*, *24*(1), 224-229. doi:10.1007/s10854-012-0716-7
12. Solomon S., Santha N., Jawahar I.N., Sreemoolanadhan H., Sebastian M.T., Mohanan P. (2000): Tailoring the microwave dielectric properties of $BaRE_2Ti_4O_{12}$ and $BaRE_2Ti_5O_{14}$ ceramics by compositional variations. *Journal of Materials Science: Materials in Electronics*, *11*(8), 595-602. doi:10.1023/A:1008924611465
13. Laffez P., Desgardin G., Raveau B. (1995): Microwave dielectric properties of doped Ba_{6-x} $(Sm_{1-y'}Nd_y)_{8+2x/3}Ti_{18}O_{54}$ oxides. *Journal of materials science*, *30*(1), 267-273. doi:10.1007/BF00352161
14. Shannon R.T., Prewitt C.T. (1969): Effective ionic radii in oxides and fluorides. *Acta Crystallographica Section B: Structural Crystallography and Crystal Chemistry*, *25*(5), 925-946. doi:10.1107/S0567740869003220
15. Klotzsche G., Windsch W., Wojcik K. (1993): Electron paramagnetic resonance investigations on manganese doped $PbTiO_3$, ceramics and single crystals. *Ferroelectrics Letters Section*, *15*(5-6), 115-120. doi:10.1080/07315179308204247
16. Hu M.Z., Qian J., Gu H.S., Hao Y. D. (2006): Phase formation, sintering behavior and microwave dielectric properties of bismuth and manganese co-doped [(Pb, Ca) La](Fe, Nb) $O_{3+\delta}$ solid solution. Journal of materials science, 41(19), 6260-6265. doi:10.1007/s10853-006-0367-2
17. Appel C.C., Bonanos N. (1999): Structural and electrical characterisation of silica-containing yttria-stabilised zirconia. *Journal of the European Ceramic Society*, *19*(6), 847-851. doi:10.1016/S0955-2219(98)00329-X
18. Hakki B.W., Coleman P.D. (1960): A dielectric resonator method of measuring inductive capacities in the millimeter range. *Microwave Theory and Techniques, IRE Transactions on*, *8*(4), 402-410. doi:10.1109/TMTT.1960.1124749
19. Tang B., Fang Z.X., Li H., Liu L., Zhang S.R. (2015): Microwave dielectric properties of H_3BO_3-doped $Ca_{0.61}La_{0.39}Al_{0.39}Ti_{0.61}O_3$ ceramics. *Journal of Materials Science: Materials in Electronics*, *26*(1), 300-306. doi:10.1007/s10854-014-2399-8
20. Liu T., Zhao X.Z., Chen W. (2006): A/B site modified $CaTiO_3$ dielectric ceramics for microwave application. *Journal of the American Ceramic Society*, *89*(3), 1153-1155. doi:10.1111/j.1551-2916.2005.00894.x
21. Zhou D., Pang L.X., Qi Z.M. (2014): Crystal Structure and Microwave Dielectric Behaviors of Ultra-Low-Temperature Fired x$(Ag_{0.5}Bi_{0.5})$ MoO_4–(1–x) $BiVO_4$ $(0.0 \leq x \leq 1.0)$ Solid Solution with Scheelite Structure. *Inorganic chemistry*, *53*(17), 9222-9227. doi:10.1021/ic501306n
22. Fang Z., Tang B., Li Y., Si F., Zhang S. (2015): Microstructures and Microwave Dielectric Properties of $Na_{0.5}Nd_{0.2}Sm_{0.3}Ti_{1-x}$ Sn_xO_3 Ceramics (x = 0.00 to 0.50). *Journal of Electronic Materials*, *44*(11), 4236-4242. doi:0.1007/s11664-015-3928-9
23. Nomura S., Tomaya K., Kaneta K. (1983): Effect of Mn doping on the dielectric properties of $Ba_2Ti_9O_{20}$ ceramics at microwave frequency. *Japanese Journal of Applied Physics*, *22*(7R), 1125. doi:10.1143/JJAP.22.1125
24. Yu S., Zhang S., Tang B., Zhou X., Fang Y. (2012): Microwave dielectric properties of BaO–2 (1−x) ZnO–$x$$Nd_2O_3$–$4TiO_2$ (x=0–1.0) ceramics. *Ceramics International*, *38*(1), 613-618. doi:10.1016/j.ceramint.2011.07.050
25. Sohn J.H., Inaguma Y., Yoon S.O., Itoh M., Nakamura T., Yoon S.J., Kim H. J. (1994): Microwave dielectric characteristics of ilmenite-type titanates with high Q values. *Japanese journal of applied physics*, *33*(9S), 5466. doi:10.1143/JJAP.33.5466
26. Fang L., Tang Y., Chu D., Zhou H., Zhang H., Chen X., Liu Q. (2012): Effect of B_2O_3 addition on the microstructure and microwave dielectric properties of $Li_2CoTi_3O_8$ ceramics. *Journal of Materials Science: Materials in Electronics*, *23*(2), 478-483. doi:10.1007/s10854-011-0421-y
27. Zhou H.F., Wang H., Zhou D., Pang L.X., Yao X. (2008): Effect of ZnO and B_2O_3 on the sintering temperature and microwave dielectric properties of $LiNb_{0.6}Ti_{0.5}O_3$ ceramics. *Materials Chemistry and Physics*, *109*(2), 510-514. doi:10.1016/j.matchemphys.2007.12.027
28. Kim J.S., Cheon C.I., Park T.R., Shim H.S. (2000): Dielectric properties and crystal structure of Ba_{6-3x} $(Nd, M)_{8+2x}Ti_{18}O_{54}$ (M = La, Bi, Y) microwave ceramics. *Journal of materials science*, *35*(6), 1487-1494. doi: 10.1023/A:1004733014635